

## Vibration of antisymmetric angle-ply laminated plates under higher order shear theory

Saira Javed<sup>1,2</sup>, K.K. Viswanathan<sup>\*1,2,3</sup>, Z.A. Aziz<sup>1,2</sup>, K. Karthik<sup>1,2</sup> and J.H. Lee<sup>4</sup>

<sup>1</sup> UTM Centre for Industrial and Applied Mathematics (UTM-CIAM), Ibnu Sina Institute for Scientific & Industrial Research, Universiti Teknologi Malaysia, 81310 Johor Bahru, Johor, Malaysia

<sup>2</sup> Department of Mathematical Sciences, Faculty of Science Universiti Teknologi Malaysia, 81310 Johor Bahru, Johor, Malaysia

<sup>3</sup> Kuwait College of Science and Technology, Doha Area, 7th Ring Road, P.O. Box No. 27235, Safat 13133, Kuwait

<sup>4</sup> Department of Naval Architecture & Ocean Engineering, Inha University, Incheon, South Korea

(Received May 09, 2016, Revised October 24, 2016, Accepted November 18, 2016)

**Abstract.** This paper deals with the analysis of vibration of antisymmetric angle-ply plates using spline method for higher order shear theory. Free vibration of laminated plates is addressed to show the capability of the present method in the vicinity of higher order shear deformation theory and simply supported edges of plates. The coupled differential equations are obtained in terms displacement and rotational functions. These displacement and rotational functions are approximated using cubic and quantic spline. A generalized eigenvalue problem is obtained and solved numerically for an eigenfrequency parameter and an associated eigenvector of spline coefficients. The antisymmetric angle-ply fiber orientation are taken as design variables. Numerical results enable us to examine the frequencies for various geometric and material parameters and accuracy and effectiveness of the proposed method is also verified by comparative study.

**Keywords:** antisymmetric angle-ply; free vibration; shear deformation theory; spline approximation; eigenvalue

### 1. Introduction

Laminated composite plates are extensively been used in civil and aerospace engineering. The attractive features of using laminated composites is because they possess numerous favourable mechanical properties such as high stiffness to weight and low density, which is particularly useful for aerospace and submarine structures because they require high stiffness and light weight. To use laminated plates structures efficiently, it is necessary to develop appropriate theories (Pagano 1970, Ferreira 2005) to predict accurately their structural and dynamic behaviour. The 3D elasticity theory was proposed by Noor (1973) to improve the accuracy of transverse shear stresses. While calculating 3D continuum elements for describing the response of thin structures, the computational cost become a serious issue. Single layer plate theories were proposed to reduce the computational cost and to convert 3D problem into 2D problem. Moreover, several laminated

---

\*Corresponding author, Associate Professor, E-mail: visu20@yahoo.com; viswanathan@utm.my

plates theories were developed. Among them classical laminated plate theory (CLPT) capable of measuring the stresses of thin composite plates while ignoring the transverse shear deformation (Reissner and Stavsky 1961). The first order shear deformation theory (FSDT) (Reissner 1972) was developed to measure the stresses of thin and moderately thick plates. According to this theory the transverse shear stresses are constant through the thickness of the plate and a shear correction factor were introduce to correct the discrepancy in the shear forces of FSDT and 3D elasticity theory (Pai and Schulz 1999). Shear correction factor depends upon the laying angle, material constants, geometry and boundary conditions, thus making this factor difficult to determine (Mackerle 2002, Yang *et al.* 2000). To overcome the discrepancies of the FSDT, higher-order shear deformation theories (HSDT) were developed to accurately evaluate the transverse shear stresses which effectively exist in thick plates. In higher-order plate theories the displacements are expanded up to any desired degree in terms of thickness coordinates (Vinson 2001, Noor *et al.* 1996) which avoid the need for a shear correction factor. Further, HSDT yields more accurate inter-laminar stress distributions and satisfies the conditions of zero shear stress at the top and bottom surfaces of the plate. In third-order plate theory the displacement are expanded up to the cubic term in thickness coordinates to have quadratic variation of transverse shear strains and transverse shear stresses through the plate thickness. This avoid the need for shear correction coefficient (Reddy 2006).

Higher-order shear deformation theory was used by Ferreira *et al.* (2003) to analyse the composite plates using multiquadric radial basis function. Neves *et al.* (2013) investigated the static, free and buckling analysis of plates using quasi 3-D higher-order shear deformation theory. Static inconsistencies of beams, plates and shells were investigated using higher-order shear deformation theory by Groh and Weaver (2015). Khandelwal *et al.* (2015) studied the vibration response of laminated composite plates with weakly boded layers. Free vibration of composite plates using higher-order shear deformation theory was investigated by Kant and Swaminathan (2001, 2002). Naserian-Nik and Tahani (2010) analysed free vibration of moderately thick rectangular laminated composite plates using semi-analytical method under different boundary conditions. Static and dynamic analysis of sandwich and laminated composite plates and shells were analysed using higher-order shear deformation theory by Mantari *et al.* (2011, 2012). Recently, Mantari and Granados (2015) examine the thermoelastic analysis of sandwich plates using quasi 3-D hybrid type HSDT. Further, Mantari and Soares (2015) used hybrid-type quasi-3D HSDT to analyse advanced composite plates. Pekovic *et al.* (2014) studied the bending analysis of composite plates under higher-order shear deformation theory. Phung-Van *et al.* (2015a) analyze cell-based three-node Mindline plate using  $C^0$ -type higher-order shear deformation for geometrically non linear analysis of composite plates. In another paper Phung-Van *et al.* (2015b) analyse composite plates having piezoelectric sensors and actuators using HSDT. Thai *et al.* (2015) studied the isogeometric analysis of composite plates using HSDT.  $C^0$ -type higher-order shear deformation theory was used for analysing laminated plates by Tran *et al.* (2015). Zhen and Wanji (2006) investigated the free vibration of laminated and sandwich plates using global-local higher-order shear deformation theory. Reddy's higher-order theory was used to examine the free vibration of composite sandwich plates by Nayak *et al.* (2002). Zuo *et al.* (2014, 2015) analysed the composite plates using wavelet finite element method and higher-order plate theory. A refined laminated plate theory was used by Wang and Shi (2015) to account the third order shear deformation and interlaminar transverse stress. Yang *et al.* (2013) conducted free vibration and buckling analysis of plates based on Reissner-Mindlin theory using a finite element method (FEM) of B-spline wavelet on the interval (BSWI).

This paper aims to investigate the free vibration of anti-symmetric angle-ply laminated plates using higher-order shear deformation theory and applying spline approximation technique. The plates kinematics is based on third order shear deformation theory (TSDT). The displacement and rotational functions are predicted using spline approximation of suitable order. Collocation with these splines yields a set of field equations which along with the equations of boundary conditions, reduce to system of homogeneous simultaneous algebraic equations on the assumed spline coefficients. Then the problem is solved using eigensolution technique to obtain the frequency parameter. The eigenvector are the spline coefficients from which the mode shapes can be constructed. The simply supported boundary condition is considered to show the parametric effects of plate's aspect ratio, side-to-thickness ratio, laying angle, number of lamina and different lamination materials on the frequency of the plate. The obtained results are presented in graphs and tables.

## 2. Formulation

The displacement field considered according to third order shear deformation theory (Reddy 2006).

$$\begin{aligned} u(x, y, z, t) &= u_0(x, y, t) + z\phi_x(x, y, t) - \frac{4z^3}{3h^2} \left( \phi_x + \frac{\partial w_0}{\partial x} \right) \\ v(x, y, z, t) &= v_0(x, y, t) + z\phi_y(x, y, t) - \frac{4z^3}{3h^2} \left( \phi_y + \frac{\partial w_0}{\partial y} \right), \quad w(x, y, z, t) = w_0(x, y, t) \end{aligned} \quad (1)$$

where  $u$ ,  $v$  and  $w$  are the displacement components in the  $x$ ,  $y$  and  $z$  directions respectively,  $u_0$  and  $v_0$  and  $w_0$  are the in-plane displacements of the middle plane and  $\phi_x$  and  $\phi_y$  are the shear rotations of any point on the middle surface of the plate.

### 2.1 Kinematics

In-plane strains are defined as

$$\boldsymbol{\varepsilon} = \begin{Bmatrix} \varepsilon_x \\ \varepsilon_y \\ \gamma_{xy} \end{Bmatrix}, \quad \boldsymbol{\varepsilon} = \boldsymbol{\varepsilon}^0 + z\boldsymbol{\varepsilon}^1 + z^3\boldsymbol{\varepsilon}^3 \quad (2)$$

where

$$\boldsymbol{\varepsilon}^0 = \begin{Bmatrix} \varepsilon_x^0 \\ \varepsilon_y^0 \\ \gamma_{xy}^0 \end{Bmatrix} = \begin{Bmatrix} \frac{\partial u_0}{\partial x} \\ \frac{\partial v_0}{\partial y} \\ \frac{\partial u_0}{\partial y} + \frac{\partial v_0}{\partial x} \end{Bmatrix}, \quad \boldsymbol{\varepsilon}^1 = \begin{Bmatrix} \varepsilon_x^1 \\ \varepsilon_y^1 \\ \gamma_{xy}^1 \end{Bmatrix} = \begin{Bmatrix} \frac{\partial \phi_x}{\partial x} \\ \frac{\partial \phi_y}{\partial y} \\ \frac{\partial \phi_x}{\partial y} + \frac{\partial \phi_y}{\partial x} \end{Bmatrix}, \quad \boldsymbol{\varepsilon}^3 = \begin{Bmatrix} \varepsilon_x^3 \\ \varepsilon_y^3 \\ \gamma_{xy}^3 \end{Bmatrix} = \left( -\frac{4}{3h^2} \right) \begin{Bmatrix} \frac{\partial \phi_x}{\partial x} + \frac{\partial^2 w_0}{\partial x^2} \\ \frac{\partial \phi_y}{\partial y} + \frac{\partial^2 w_0}{\partial y^2} \\ \frac{\partial \phi_x}{\partial y} + \frac{\partial \phi_y}{\partial x} + 2\frac{\partial^2 w_0}{\partial x \partial y} \end{Bmatrix}$$

and the shear strain components are defined as

$$\gamma = \begin{Bmatrix} \gamma_{yz} \\ \gamma_{xz} \end{Bmatrix}, \quad \gamma = \gamma^0 + z^2 \gamma^2 \quad (3)$$

where

$$\gamma^0 = \begin{Bmatrix} \gamma_{yz}^0 \\ \gamma_{xz}^0 \end{Bmatrix} = \begin{Bmatrix} \phi_y + \frac{\partial w_0}{\partial y} \\ \phi_x + \frac{\partial w_0}{\partial x} \end{Bmatrix}, \quad \gamma^2 = \begin{Bmatrix} \gamma_{yz}^2 \\ \gamma_{xz}^2 \end{Bmatrix} = \left( -\frac{4}{h^2} \right) \begin{Bmatrix} \phi_y + \frac{\partial w_0}{\partial y} \\ \phi_x + \frac{\partial w_0}{\partial x} \end{Bmatrix}$$

## 2.2 Constitutive equations

The stress-strain relations for the  $k$ -th layer, after neglecting transverse normal strain and stress, are of the form

$$\begin{pmatrix} \sigma_x^{(k)} \\ \sigma_y^{(k)} \\ \tau_{xy}^{(k)} \\ \tau_{yz}^{(k)} \\ \tau_{xz}^{(k)} \end{pmatrix} = \begin{pmatrix} C_{11}^{(k)} & C_{12}^{(k)} & C_{16}^{(k)} & 0 & 0 \\ C_{12}^{(k)} & C_{22}^{(k)} & C_{26}^{(k)} & 0 & 0 \\ C_{16}^{(k)} & C_{26}^{(k)} & C_{66}^{(k)} & 0 & 0 \\ 0 & 0 & 0 & C_{44}^{(k)} & C_{45}^{(k)} \\ 0 & 0 & 0 & C_{45}^{(k)} & C_{55}^{(k)} \end{pmatrix} \begin{pmatrix} \varepsilon_x^{(k)} \\ \varepsilon_y^{(k)} \\ \gamma_{xy}^{(k)} \\ \gamma_{yz}^{(k)} \\ \gamma_{xz}^{(k)} \end{pmatrix} \quad (4)$$

When the materials are oriented at an angle  $\theta$  with the  $x$ -axis, the transformed stress-strain relations are

$$\begin{pmatrix} \sigma_x^{(k)} \\ \sigma_y^{(k)} \\ \tau_{xy}^{(k)} \\ \tau_{yz}^{(k)} \\ \tau_{xz}^{(k)} \end{pmatrix} = \begin{pmatrix} Q_{11}^{(k)} & Q_{12}^{(k)} & Q_{16}^{(k)} & 0 & 0 \\ Q_{12}^{(k)} & Q_{22}^{(k)} & Q_{26}^{(k)} & 0 & 0 \\ Q_{16}^{(k)} & Q_{26}^{(k)} & Q_{66}^{(k)} & 0 & 0 \\ 0 & 0 & 0 & Q_{44}^{(k)} & Q_{45}^{(k)} \\ 0 & 0 & 0 & Q_{45}^{(k)} & Q_{55}^{(k)} \end{pmatrix} \begin{pmatrix} \varepsilon_x^{(k)} \\ \varepsilon_y^{(k)} \\ \gamma_{xy}^{(k)} \\ \gamma_{yz}^{(k)} \\ \gamma_{xz}^{(k)} \end{pmatrix} \quad (5)$$

where  $Q_{ij}^{(k)}$ , as functions of  $C_{ij}^{(k)}$  are fully furnished in Viswanathan and Lee (2007). The stress resultants are defined as

$$\begin{Bmatrix} N_i \\ M_i \\ P_i \end{Bmatrix} = \int_{-h/2}^{h/2} \sigma_i \begin{Bmatrix} 1 \\ z \\ z^3 \end{Bmatrix} dz, \quad \begin{Bmatrix} Q_i \\ R_i \end{Bmatrix} = \int_{-h/2}^{h/2} \tau_i \begin{Bmatrix} 1 \\ z^2 \end{Bmatrix} dz \quad (6)$$

where  $N_i$ ,  $M_i$  and  $Q_i$  are stress, moment and shear resultants respectively.  $P_i$  and  $R_i$  denote higher-order stress resultants. The stress-strain relations are obtained as follows

$$\begin{pmatrix} N \\ M \\ P \\ Q \\ R \end{pmatrix} = \begin{pmatrix} A & B & E & 0 & 0 \\ B & D & F & 0 & 0 \\ E & F & H & 0 & 0 \\ 0 & 0 & 0 & A' & D' \\ 0 & 0 & 0 & D' & F' \end{pmatrix} \begin{pmatrix} \varepsilon^0 \\ \varepsilon^1 \\ \varepsilon^3 \\ \gamma^0 \\ \gamma^2 \end{pmatrix} \quad (7)$$

Stiffness coefficients are defined as

$$\begin{aligned} A_{ij} &= \sum_k \bar{Q}_{ij}^{(k)} (z_k - z_{k-1}), & B_{ij} &= \frac{1}{2} \sum_k \bar{Q}_{ij}^{(k)} (z_k^2 - z_{k-1}^2), & D_{ij} &= \frac{1}{3} \sum_k \bar{Q}_{ij}^{(k)} (z_k^3 - z_{k-1}^3) \\ E_{ij} &= \frac{1}{4} \sum_k \bar{Q}_{ij}^{(k)} (z_k^4 - z_{k-1}^4), & F_{ij} &= \frac{1}{5} \sum_k \bar{Q}_{ij}^{(k)} (z_k^5 - z_{k-1}^5), & H_{ij} &= \frac{1}{7} \sum_k \bar{Q}_{ij}^{(k)} (z_k^7 - z_{k-1}^7) \end{aligned} \quad (8)$$

for  $i, j = 1, 2, 6$

$$A'_{ij} = \sum_k \bar{Q}_{ij}^{(k)} (z_k - z_{k-1}), \quad D'_{ij} = \frac{1}{3} \sum_k \bar{Q}_{ij}^{(k)} (z_k^3 - z_{k-1}^3) \quad \text{and} \quad F'_{ij} = \frac{1}{5} \sum_k \bar{Q}_{ij}^{(k)} (z_k^5 - z_{k-1}^5)$$

for  $i, j = 4, 5$  where the elastic coefficients  $A_{ij}$ ,  $B_{ij}$  and  $D_{ij}$  (extensional, bending-extensional coupling and bending stiffnesses) and  $E_{ij}$ ,  $F_{ij}$  and  $H_{ij}$  are the higher-order stiffness coefficients. The equilibrium equations considered are as follows

$$\begin{aligned} \frac{\partial N_x}{\partial x} + \frac{\partial N_{xy}}{\partial y} &= I_0 \frac{\partial^2 u}{\partial t^2}, & \frac{\partial N_{xy}}{\partial x} + \frac{\partial N_y}{\partial y} &= I_0 \frac{\partial^2 v}{\partial t^2} \\ \frac{\partial \bar{Q}_x}{\partial x} + \frac{\partial \bar{Q}_y}{\partial y} + c_1 \left( \frac{\partial^2 P_x}{\partial x^2} + 2 \frac{\partial^2 P_{xy}}{\partial x \partial y} + \frac{\partial^2 P_y}{\partial y^2} \right) & \\ = I_0 \frac{\partial^2 w}{\partial t^2} - c_1^2 I_6 \left( \frac{\partial^4 w_0}{\partial x^2 \partial t^2} + \frac{\partial^4 w_0}{\partial y^2 \partial t^2} \right) + c_1 J_4 \left( \frac{\partial^3 \phi_x}{\partial x \partial t^2} + \frac{\partial^3 \phi_y}{\partial y \partial t^2} \right) & \\ \frac{\partial \bar{M}_{xx}}{\partial x} + \frac{\partial \bar{M}_{xy}}{\partial y} - \bar{Q}_x &= K_2 \frac{\partial^2 \phi_x}{\partial t^2} - c_1 J_4 \frac{\partial^3 w}{\partial x \partial t^2}, & \frac{\partial \bar{M}_{xy}}{\partial x} + \frac{\partial \bar{M}_{yy}}{\partial y} - \bar{Q}_y &= K_2 \frac{\partial^2 \phi_y}{\partial t^2} - c_1 J_4 \frac{\partial^3 w}{\partial y \partial t^2} \end{aligned} \quad (9)$$

Here

$$I_i = \int_z \rho^{(k)}(z)^i dz \quad (i = 0, 1, 2, 3, \dots, 6)$$

and  $\rho$  is the material density of the  $k$ -th layer and

$$\bar{M}_{\alpha\beta} = M_{\alpha\beta} - c_1 P_{\alpha\beta}, \quad \bar{Q}_\alpha = Q_\alpha - c_2 R_\alpha, \quad J_i = I_i - c_1 I_{i+2}, \quad K_2 = I_2 - 2c_1 I_4 + c_1^2 I_6.$$

Substitute Eqs. (2) and (3) into Eq. (7) and then substituting into Eq. (9). Further, equating the following laminate stiffnesses equal to zero for anti-symmetric angle-ply laminates (Reddy 1997)

$$A_{16}, A_{26}, A_{45}, B_{11}, B_{12}, B_{22}, B_{66}, D_{16}, D_{26}, D_{45}, E_{11}, E_{12}, E_{22}, E_{66}, H_{16}, H_{26}, F_{16}, F_{26}, F_{45} = 0.$$

The displacements and rotational functions are assumed in the separable form for antisymmetric angle-ply plates as

$$\begin{aligned} u(x, y) &= U(x) \cos \frac{n\pi y}{b} e^{i\omega t} \\ v(x, y) &= V(x) \sin \frac{n\pi y}{b} e^{i\omega t} \\ w(x, y) &= W(x) \sin \frac{n\pi y}{b} e^{i\omega t} \\ \phi_x(x, y) &= \Phi_x(x) \sin \frac{n\pi y}{b} e^{i\omega t} \\ \phi_y(x, y) &= \Phi_y(x) \cos \frac{n\pi y}{b} e^{i\omega t} \end{aligned} \quad (10)$$

The non-dimensional parameters introduced are as follows

$$\lambda = \omega a \sqrt{\frac{I_0}{A_{11}}}, \text{ a frequency parameter}$$

$$\delta_k = \frac{h_k}{h}, \quad \text{the relative layer thickness of the k-th layer}$$

$$\phi = \frac{a}{b}, \quad \text{aspect ratio}$$

$$X = \frac{x}{a}, \quad \text{a distance coordinate}$$

$$H = \frac{a}{h}, \quad \text{side-to-thickness ratio}$$

Using Eq. (10) and introducing non-dimensional parameters, modified equations in the matrix form are obtained as

$$\begin{bmatrix} L_{11} & L_{12} & L_{13} & L_{14} & L_{15} \\ L_{21} & L_{22} & L_{23} & L_{24} & L_{25} \\ L_{31} & L_{32} & L_{33} & L_{34} & L_{35} \\ L_{41} & L_{42} & L_{43} & L_{44} & L_{45} \\ L_{51} & L_{52} & L_{53} & L_{54} & L_{55} \end{bmatrix} \begin{Bmatrix} U \\ V \\ W \\ \Phi_x \\ \Phi_y \end{Bmatrix} = \begin{Bmatrix} 0 \\ 0 \\ 0 \\ 0 \\ 0 \end{Bmatrix} \quad (11)$$

where  $L_{ij}'$ s are shown in Appendix.

### 2.3 Method of solution

The differential equations in Eq. (11) contain derivatives of second order in  $U(X)$ , third order in  $V(X)$ , fourth order in  $W(X)$ , third order in  $\Phi_X(X)$  and second order in  $\Phi_Y(X)$ . These functions are approximated by using cubic and quantic spline functions, in the range of  $X \in [0, 1]$ , since splines are relatively simple and elegant and use series of lower order approximations rather than global higher order approximations, affording fast convergence and high accuracy.

The displacement functions  $U(X)$ ,  $V(X)$  and  $W(X)$  and the rotational functions  $\Phi_X(X)$   $\Phi_Y(X)$  are approximated respectively by the splines

$$\begin{aligned} U(X) &= \sum_{i=0}^2 a_i X^i + \sum_{j=0}^{N-1} b_j (X - X_j)^3 H(X - X_j) \\ V(X) &= \sum_{i=0}^4 c_i X^i + \sum_{j=0}^{N-1} d_j (X - X_j)^5 H(X - X_j) \\ W(X) &= \sum_{i=0}^4 e_i X^i + \sum_{j=0}^{N-1} f_j (X - X_j)^5 H(X - X_j) \\ \Phi_X(X) &= \sum_{i=0}^4 g_i X^i + \sum_{j=0}^{N-1} p_j (X - X_j)^5 H(X - X_j) \\ \Phi_Y^*(X) &= \sum_{i=0}^2 l_i X^i + \sum_{j=0}^{N-1} q_j (X - X_j)^3 H(X - X_j) \end{aligned} \quad (12)$$

Here  $H(X - X_j)$  is the Heaviside step function and  $N$  is the number of intervals into which the range  $[0, 1]$  of  $X$  is divided. The points  $X = X_s = \frac{s}{N}$ , ( $s = 0, 1, 2, \dots, N$ ) are chosen as the knots of the splines, as well as the collocation points. Thus the splines are assumed to satisfy the differential equations given by Eq. (12), at all  $X_s$ . The resulting expressions contain  $(5N + 5)$  homogeneous system of equations in the  $(5N + 21)$  spline coefficients.

The boundary condition considered on the edges  $x = 0$  and  $x = a$  are

(1) (S-S): both the ends simply supported

This boundary condition gives 13 more equations, thus making a total of  $(5N + 18)$  equations, in the same number of unknowns. The resulting field and boundary condition equations may be written in the form

$$[M]\{q\} = \lambda^2 [P]\{q\} \quad (13)$$

where  $[M]$  and  $[P]$  are square matrices,  $\{q\}$  is a column matrix. This is treated as a generalized eigenvalue problem in the eigenparameter  $\lambda$  and the eigenvector  $\{q\}$  whose elements are the spline coefficients.

### 3. Results and discussion

The higher order shear deformation theory is used to investigate the free vibration of anti-symmetric angle-ply plates for simply supported end condition. All numerical computations in this section, unless otherwise stated, two materials are considered: Kevlar-49/epoxy (KE) and Graphite/Epoxy (AS4/3501-6) (GE). Two, four, and six layered plates with anti-symmetric angle-ply orientations are considered.

#### 3.1 Convergence study

The frequency parameter with respect to different configurations are carried out to confirm the convergence of the spline method for antisymmetric angle-ply plates. The number of subintervals  $N$  of the range  $X \in [0, 1]$ . The value of  $N$  started from 4 and finally it is fixed for  $N = 18$ , since for the next value of  $N$ , the percent changes in the values of  $\lambda$  are very low, the maximum being 3%.

#### 3.2 Validation

The accuracy and effectiveness of the proposed method is verified with the number of previous studies available in the literature. Table 1 shows the comparison of the fundamental frequency with respect to the side-to-thickness ratio and aspect ratio of the present results compared with Swaminathan and Patil (2008a), for two layered antisymmetric angle-ply square laminated plates under higher order shear deformation theory. It can be seen from the Table 1, some of the present values closer and few values are significantly lesser than the results obtained by Swaminathan and Patil (2008a). Table 2 depicts the comparison of fundamental frequencies of four layered anti

Table 1 Non-dimensioned fundamental frequencies for simply supported two layered antisymmetric angles-ply ( $\theta/\theta$ ) square laminated plate

$$\bar{\omega} = (\omega b^2 / h) \sqrt{\rho / E_2}, \quad E_1/E_2 = 40, \quad G_{12}/E_2 = G_{13}/E_2 = 0.6, \quad G_{23}/E_2 = 0.5, \quad \nu_{12} = \nu_{13} = \nu_{23} = 0.25$$

$\theta$	Source	a/h	
		2	4
15°	Present	4.8711	8.3495
	Swaminathan and Patil (2008a)	Model 1	5.1600
		Model 2	5.1390
		Model 3	5.6280
		Model 4	5.9909
	a/b		
	1		
	Present	8.3495	3.8611
	Swaminathan and Patil (2008a)	Model 1	8.5142
		Model 2	8.4789
		Model 3	8.8117
		Model 4	9.4119



Table 2 Non-dimensionalized fundamental frequencies for simply supported four layered antisymmetric angle-ply (45°/–45°/45°/–45°) square laminated plate

$$\bar{\omega} = (\omega b^2 / h) \sqrt{\rho / E_2}, \quad E_1 / E_2 = 40, \quad G_{12} / E_2 = G_{13} / E_2 = 0.6, \quad G_{23} / E_2 = 0.5, \quad \nu_{12} = \nu_{13} = \nu_{23} = 0.25$$

Lamination and number of layers	Source	a/h	
		2	4
45°/–45°/45°/–45°	Present	5.7035	10.3677
	Swaminathan and Patil (2008b)	5.5674	10.0731
		6.1067	10.6507

Table 3 Fundamental frequency  $\lambda$  of four layered anti-symmetric plates (45°/–45°/45°/–45°)  $a / h = 20$

$$\lambda' = \omega a^2 \sqrt{\frac{\rho}{E_2 h^2}}, \quad E_1 / E_2 = 40, \quad G_{12} / E_2 = 0.6, \quad G_{13} / E_2 = G_{23} / E_2 = 0.5, \quad \nu_{12} = 0.25$$

Sources	a/b									
	0.2	0.4	0.6	0.8	1	1.2	1.4	1.6	1.8	2
Present	8.8974	10.2512	12.8226	15.9767	19.6810	25.6715	29.6799	33.2168	38.7031	44.7735
Ghosh and Dey (1994)	9.52	11.70	14.72	18.26	22.19	26.45	31.02	35.89	41.07	46.54
Reddy (1979)	9.475	11.767	14.896	18.557	22.584	26.857	31.401	36.249	41.372	46.789
Bert and Chen (1978)	9.300	11.46	14.45	17.97	21.87	26.12	30.68	35.56	-	46.26

Table 4 Fundamental frequency variation of four layered plates with respect to side-to-thickness ratio  $a / h = 0.4$

a/h	30°/–30°/30°/–30° (GE/GE/GE/GE)	45°/–45°/45°/–45° (GE/GE/GE/GE)	60°/–60°/60°/–60° (GE/GE/GE/GE)
10	0.7485	0.8737	1.8039
20	0.5160	0.69328	1.4055
30	0.5043	0.6218	1.1095
40	0.4837	0.5912	0.9823
50	0.4043	0.5606	0.7622
60	0.3654	0.4959	0.6133

symmetric angle-ply plates for side-to-thickness ratio fixed as 2 and 4 showing that the present results are closer to the results of Swaminathan and Patil (2008b). Table 3 presents the comparison of current results with the FSDT with the fundamental frequency  $\lambda$  for four layered anti-symmetric angle-ply plates (45°/–45°/45°/–45°). It is observed that the present results are significantly lesser than the results obtained using FSDT (Bert and Chen 1978, Ghosh and Dey 1994, Reddy 1979).

Table 4 depicts the effect of side-to-thickness ratio on the fundamental frequency of four layered plates consisting of GE material with different laying angles. The aspect ratio  $a / b = 0.4$  is

fixed. It is seen that frequency increases with the increase of laying angle. Further, frequency decreases with the increase of side-to-thickness ratio.

### 3.3 Effect of different materials and geometric parameters on the frequency of antisymmetric angle-ply plates

#### 3.3.1 Effect of aspect ratio

Fig. 1 depicts the effect of aspect ratio  $a/b$ , laying-angle and material sequence on the value of frequency parameter  $\lambda_m$  of six layered plates. The laying angle  $45^\circ/-30^\circ/60^\circ/-60^\circ/30^\circ/-45^\circ$  and

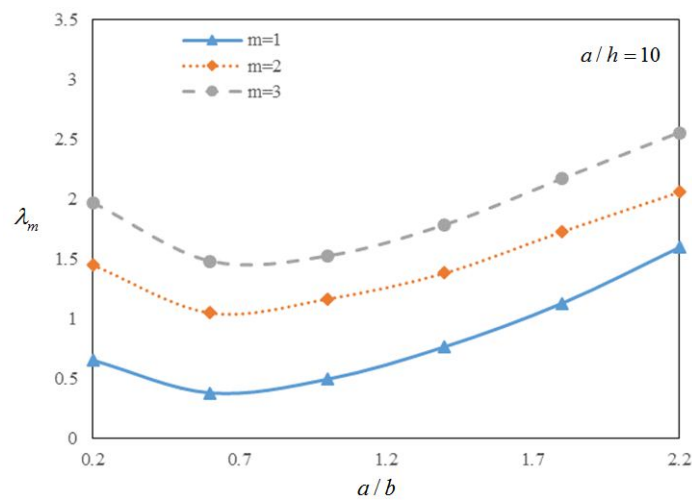


Fig. 1 The frequency variation of six layered anti-symmetric angle-ply plates with respect to aspect ratio:  $45^\circ/-30^\circ/60^\circ/-60^\circ/30^\circ/-45^\circ$  (KE/GE/KE/KE/GE/KE)

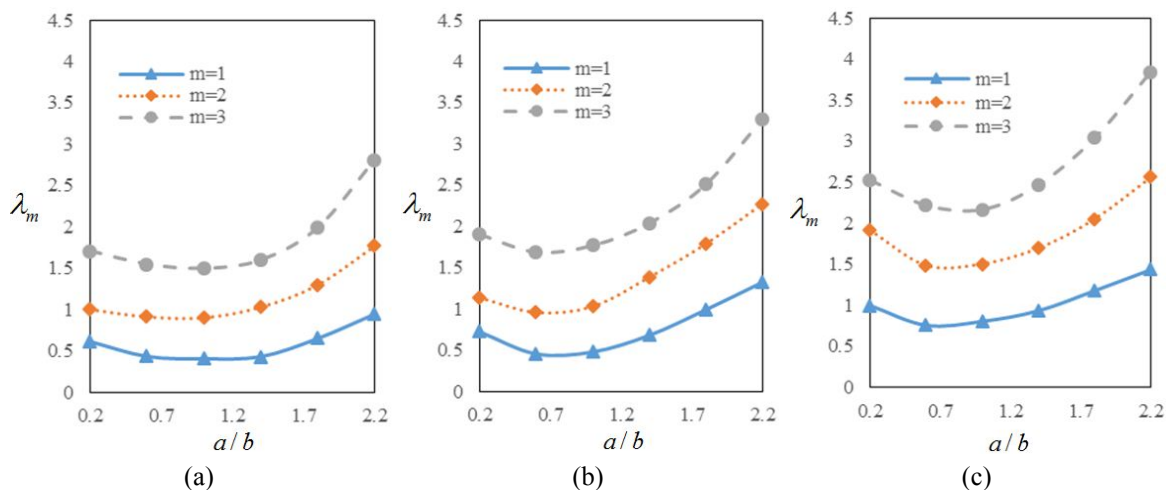


Fig. 2 The frequency variation of six layered anti-symmetric angle-ply plates with respect to aspect ratio: (a)  $30^\circ/-30^\circ/30^\circ/-30^\circ/30^\circ/-30^\circ$ ; (b)  $45^\circ/-45^\circ/45^\circ/-45^\circ/45^\circ/-45^\circ$ ; (c)  $60^\circ/-60^\circ/60^\circ/-60^\circ/60^\circ/-60^\circ$  consisting of KE material

material combination (KE/GE/KE/KE/GE/KE) is considered and side-to-thickness ratio is fixed as  $a/b = 10$ . It can be seen that the frequency value decrease slowly till  $a/b = 0.6$  and increases gradually afterwards.

The variation of frequency parameter  $\lambda_m$  with respect to the aspect ratio is shown in Fig. 2. The material values of KE is used and six layered plates with different ply angles are considered. The frequency values are decreases in the range  $0.2 < a/b < 0.6$  and slowly increases afterwards. Moreover, the frequency values are increases with increasing ply-angles.

Fig. 3 shows the variation of frequency value with respect to the aspect ratio for four layered plates with the different ply-angles consisting of materials KE and GE arranged in the order of KE/GE/GE/KE. The maximum relative values increase for the first three modes, in the range  $0.2 \leq$

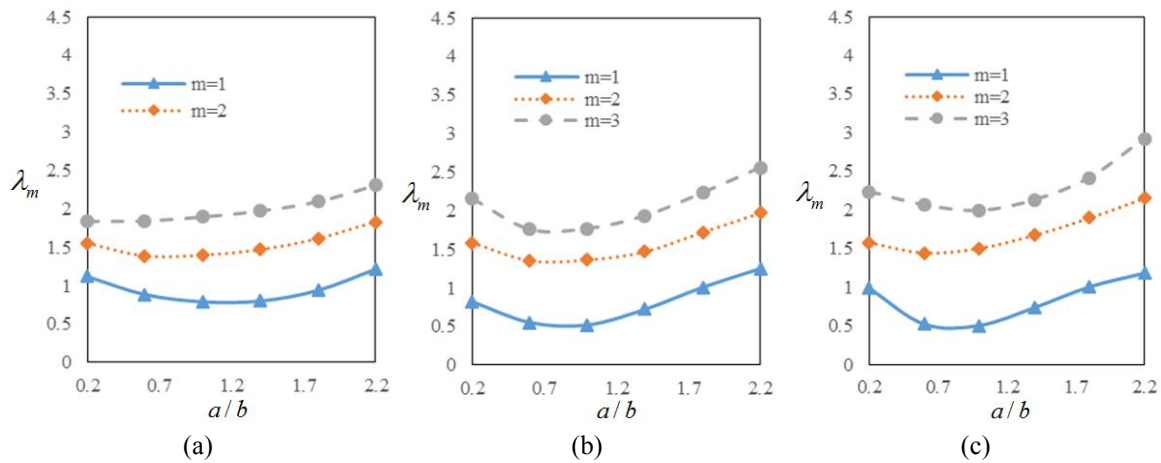


Fig. 3 The frequency variation of four layered anti-symmetric angle-ply plates with respect to aspect ratio: (a)  $30^\circ/-60^\circ/60^\circ/-30^\circ$ ; (b)  $60^\circ/-45^\circ/45^\circ/-60^\circ$ ; (c)  $45^\circ/-60^\circ/60^\circ/-45^\circ$  consisting of KE/GE/GE/KE materials combination

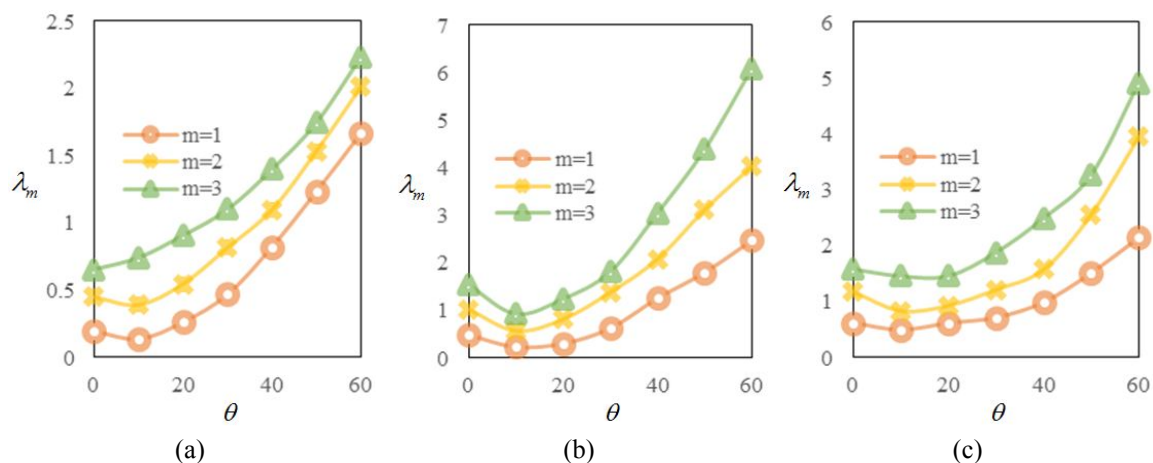


Fig. 4 The frequency variation of two layered anti-symmetric angle-ply plates with respect to laying-angle (a)  $a/b = 0.4$ ; (b)  $a/b = 1$ ; (c)  $a/b = 1.6$  consisting of KE material

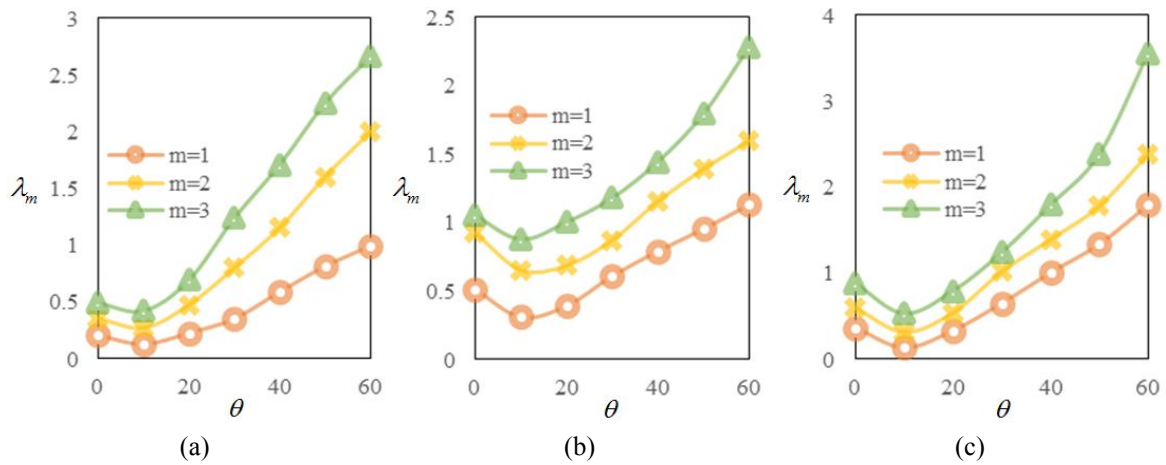


Fig. 5 The frequency variation of four layered anti-symmetric angle-ply plates with respect to laying-angle: (a)  $a/b = 0.4$ ; (b)  $a/b = 1$ ; (c)  $a/b = 1.6$  consisting of (KE/GE/GE/KE) materials combination

$(a/b) \leq 2.2$ , are 0.096119, 0.27516 and 0.467566 for Fig. 3(a), 0.426667, 0.384791 and 0.405663 for Fig. 3(b) and 0.193654, 0.578167 and 0.688356 for Fig. 3(c).

### 3.3.2 Effect of ply-angle

The effect of ply-angle  $\theta$  and aspect ratio shows that the frequency value decreases between  $0 \leq \theta \leq 20$  and significantly increases afterwards for two layered antisymmetric plates using KE material. The aspect ratio is fixed as  $a/b = 0.4$  for Fig. 4(a),  $a/b = 1$  for Fig. 4(b), and  $a/b = 1.6$  for Fig. 4(c).

Four layered anti-symmetric angle-ply plates with material combination (KE/GE/GE/KE) are considered to examine the effect of ply-angle on the value of the frequency parameter. Figure 5. shows that the frequency value inially decreases for certain value and increases afterwards. The aspect ratio is fixed as  $a/b = 0.4$  for Fig. 5(a),  $a/b = 1$  for Fig. 5(b), and  $a/b = 1.6$  for Fig. 5 (c).

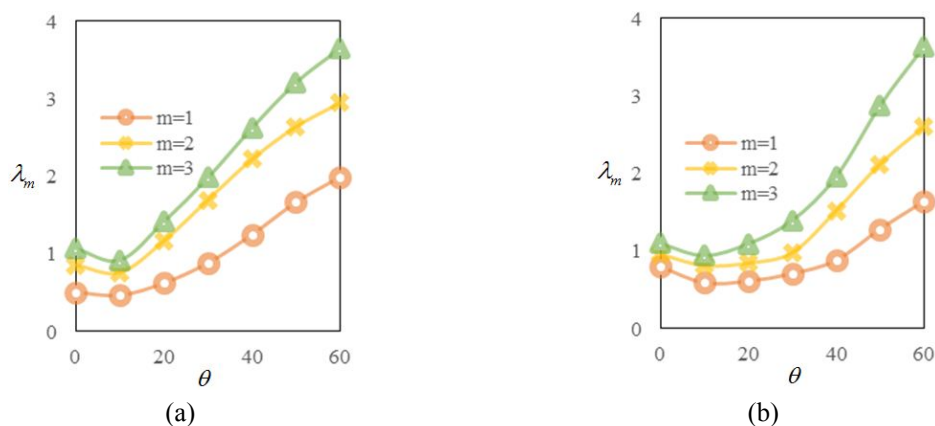


Fig. 6 The frequency variation of six layered anti-symmetric angle-ply plates with respect to laying-angle consisting of: (a) (KE/GE/KE/KE/GE/KE); (b) (GE/KE/GE/GE/KE/KE) materials combination  $a/b = 1$

Fig. 6 shows six layered antisymmetric angle-ply plates with two different material combinations are considered (KE/GE/KE/KE/GE/KE), (GE/KE/GE/GE/KE/GE). The aspect ratio is fixed as  $a/b = 1$ . It is observed that there is a decrease and then increase in the frequency values with ply-angle increases.

### 3.3.3 Effect of side-to-thickness-ratio

The variation of the frequency parameter between the range of side-to-thickness ratio  $10 \leq (a/h) \leq 60$  is presented in Fig. 7 showing that frequency value decreases strictly between  $10 \leq (a/h) \leq 20$  and decreases slowly afterwards. Six layered antisymmetric plates with laying-angle  $60^\circ/-45^\circ/30^\circ/-30^\circ/45^\circ/-60^\circ$  (GE/KE/GE/GE/KE/GE) is considered. The aspect ratio is fixed as  $a/b = 1$  and  $a/b = 1.6$  for Figs. 7(a) and (b) respectively.

Fig. 8 illustrates the effect of different material combinations and side-to-thickness ratio with ply-angle arranged as  $30^\circ/-45^\circ/60^\circ/-60^\circ/45^\circ/-30^\circ$  and material combinations for Fig. 8(a) as

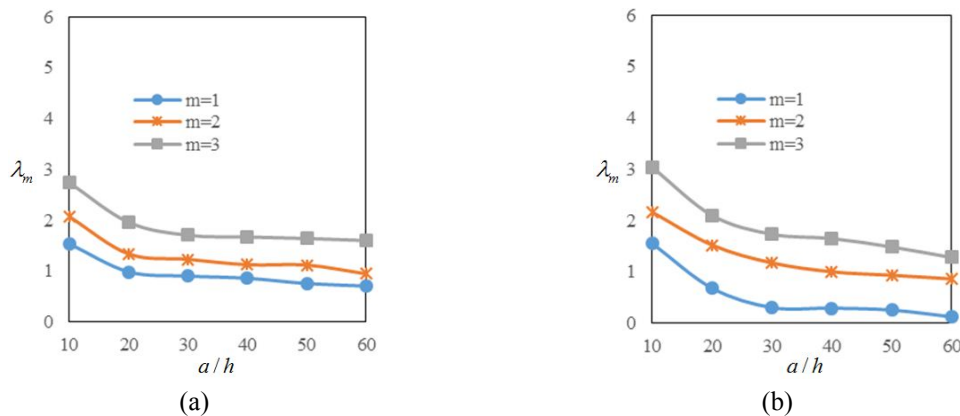


Fig. 7 The frequency variation of six layered anti-symmetric angle-ply plates with respect to side-to-thickness ratio consisting of (a)  $a/b = 1$ ; (b)  $a/b = 1.6$ , laying-angle  $60^\circ/-45^\circ/30^\circ/-30^\circ/45^\circ/-60^\circ$  materials combination (GE/KE/GE/GE/KE/GE)

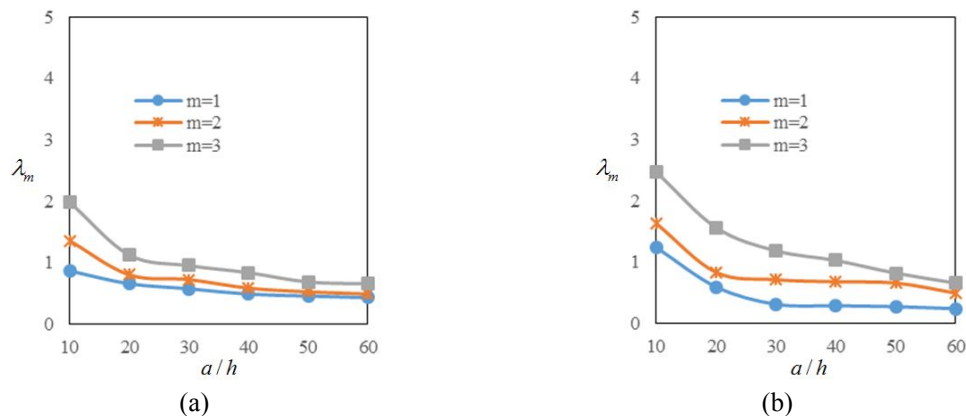


Fig. 8 The frequency variation of six layered anti-symmetric angle-ply plates with respect to side-to-thickness ratio consisting of laying-angle  $30^\circ/-45^\circ/60^\circ/-60^\circ/45^\circ/-30^\circ$ ; (a) (GE/KE/GE/GE/KE/GE); (b) (KE/GE/KE/KE/GE/KE) materials combination,  $a/b = 0.4$

(GE/KE/GE/GE/KE/GE) and Fig. 8(b) as (KE/GE/KE/KE/GE/KE) on the frequency parameter value. The aspect ratio is fixed as  $a/b = 0.4$ . It can be seen that the frequency value decreases strictly between  $10 \leq (a/h) \leq 20$  and slowly decreases afterwards.

The effect of different aspect ratio and side-to-thickness ratio on the frequency parameter value of six layered plates with laying-angle  $30^\circ/-45^\circ/60^\circ/-60^\circ/45^\circ/-30^\circ$  (KE/GE/KE/KE/GE/KE) is presented in Fig. 9. The results shows that frequency value decreases with the increase of side to thickness ratio. Further, the frequency value is higher for aspect ratio  $a/b = 1$  as compare to  $a/b = 0.4$ .

Four layered plates with anti-symmetric layers  $30^\circ/-30^\circ/30^\circ/-30^\circ$ ,  $45^\circ/-45^\circ/45^\circ/-45^\circ$  and  $60^\circ/-60^\circ/60^\circ/-60^\circ$  and material combination as (GE/KE/KE/GE) are considered in Fig. 10. The

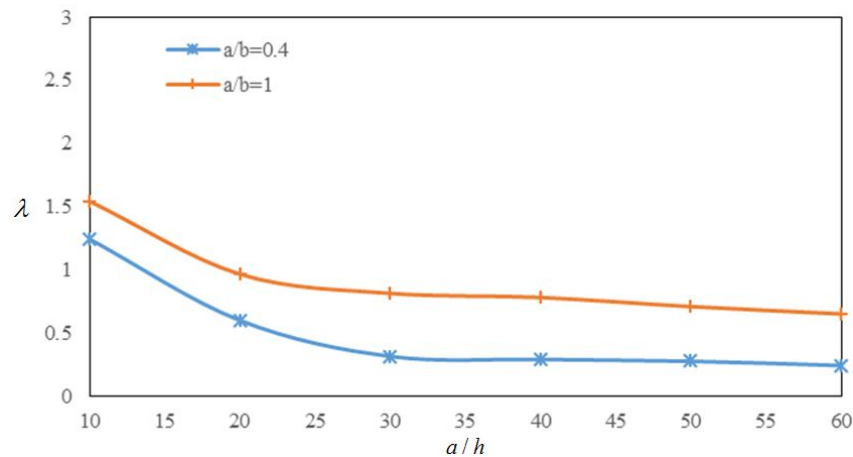


Fig. 9 The fundamental frequency variation of six layered anti-symmetric angle-ply plates with respect to side-to-thickness ratio consisting of laying-angle  $30^\circ/-45^\circ/60^\circ/-60^\circ/45^\circ/-30^\circ$  (KE/GE/KE/KE/GE/KE) materials combination: (a)  $a/b = 0.4$ ; (b)  $a/b = 1$

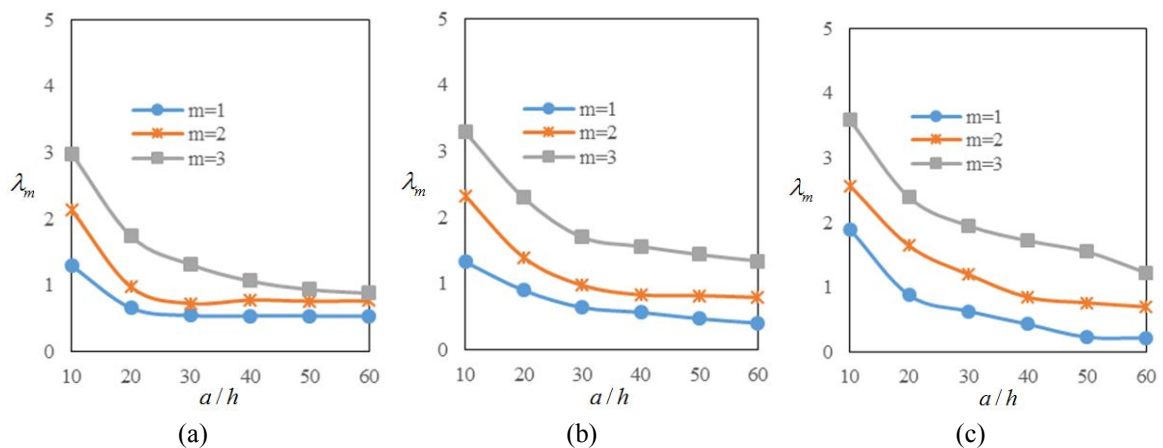


Fig. 10 The fundamental frequency variation of four layered anti-symmetric angle-ply plates with respect to side-to-thickness ratio consisting of laying-angle: (a)  $30^\circ/-30^\circ/30^\circ/-30^\circ$ ; (b)  $45^\circ/-45^\circ/45^\circ/-45^\circ$ ; (c)  $60^\circ/-60^\circ/60^\circ/-60^\circ$  (GE/KE/KE/GE) materials combination,  $a/b = 1$

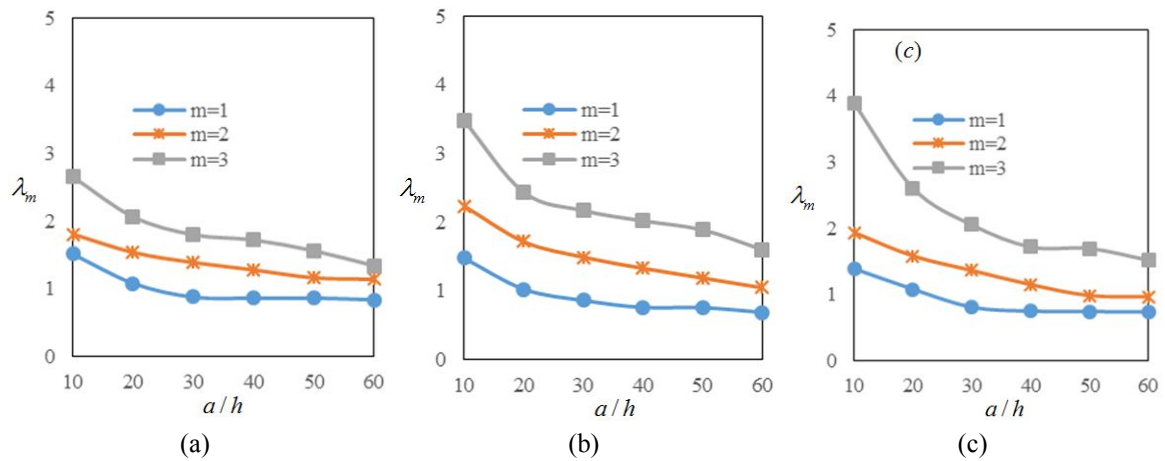


Fig. 11 The fundamental frequency variation of two layered anti-symmetric angle-ply plates with respect to side-to-thickness ratio consisting of laying-angle: (a) 30°/-30°; (b) 45°/-45°; (c) 60°/-60° (GE/GE) materials combination,  $a/b = 1$

aspect ratio is fixed as  $a/b = 1$ . The effect of side-to-thickness ratio shows that frequency decreases significantly in the beginning and decreases slowly between  $20 \leq a/b \leq 60$ . Further, it is also seen that frequency value increases with the increase of laying-angle.

The frequency variation of two layered plates with laying-angles as 30°/-30°, 45°/-45°, 60°/-60° and material combination as (GE/GE) is presented in Fig. 11. The aspect ratio is fixed as  $a/b = 1$ . It is observed that frequency decreases with the increase of side-to-thickness ratio.

#### 4. Conclusions

In this paper the free vibration of anti-symmetric angle-ply plates are analysed using spline approximation under higher-order shear deformation theory. The vibrational behavior of laminated plates is examined for simply supported boundary conditions. The vibration characteristic of the plates is examined for aspect ratio, ply-angle, side-to-thickness ratio, different number of layers and two different lamination materials. It is concluded that variation of the geometric parameters and materials effect the frequencies of plates, which may be beneficial for the designers of related fields.

#### Acknowledgments

The authors thankfully acknowledge the financial support from Ministry of Higher Education Malaysia, MOHE-GUP Project Vote No. 11H90 under Research Management Centre (RMC), Universiti Teknologi Malaysia, Johor Bahru, Malaysia.

#### References

- Bert, C.W. and Chen, T.L.C. (1978), "Effect of shear deformation on vibration of antisymmetric angle-ply laminated rectangular plates", *Int. J. Solids Struct.*, **14**(6), 465-473.



- Ferreira, A.J.M. (2005), "Analysis of composite plates using a layerwise deformation theory and multiquadrics discretization", *Mech. Adv. Mater. Struct.*, **12**(2), 99-112.
- Ferreira, A.J.M., Roque, C.M.C. and Martins, P.A.L.S. (2003), "Analysis of composite plates using higher-order shear deformation theory and a finite point formulation based on the multiquadric radial basis function method", *Compos. Part B: Eng.*, **34**(7), 627-636.
- Ghosh, A.K. and Dey, S.S. (1994), "Free vibration of laminated composite plates-a simple finite element based on higher order theory", *Comput. Struct.*, **52**(3), 397-404.
- Groh, R.M.J. and Weaver, P.M. (2015), "Static inconsistencies in certain axiomatic higher-order shear deformation theories for beams, plates and shells", *Compos. Struct.*, **120**, 231-245.
- Kant, T. and Swaminathan, K. (2001), "Free vibration of isotropic, orthotropic, and multilayer plates based on higher order refined theories", *J. Sound Vib.*, **241**(2), 319-327.
- Kant, T. and Swaminathan, K. (2002), "Analytical solutions for the static analysis of laminated composite and sandwich plates based on a higher order refined theory", *Compos. Struct.*, **56**(4), 329-344.
- Khandelwal, R.P., Chakrabarti, A. and Bhargava, P. (2015), "Vibration response of laminated composite plate having weakly bonded layers", *Appl. Math. Model.*, **39**(17), 5073-5090.
- Mackerle, J. (2002), "Finite element analyses of sandwich structures: A bibliography (1980-2001)", *Eng. Computat.*, **19**(2), 206-245.
- Mantari, J.L. and Granados, E.V. (2015), "Thermoelastic analysis of advanced sandwich plates based on a new quasi-3D hybrid type HSDT with 5 unknowns", *Compos. Part B: Eng.*, **69**, 317-334.
- Mantari J.L. and Soares, C.G. (2015), "Five-unknowns generalized hybrid-type quasi-3D HSDT for advanced composite plates", *Appl. Math. Model.*, **39**(18), 5598-5615.
- Mantari, J.L., Oktem, A.S. and Soares, C.G. (2011), "Static and dynamic analysis of laminated composite and sandwich plates and shells by using a new higher-order shear deformation theory", *Compos. Struct.*, **94**(1), 37-49.
- Mantari, J.L., Oktem, A.S. and Soares, C.G. (2012), "A new higher order shear deformation theory for sandwich and composite laminated plates", *Compos. Part B: Eng.*, **43**(3), 1489-1499.
- Naserian-Nik, A.M. and Tahani, M. (2010), "Free vibration analysis of moderately thick rectangular laminated composite plates with arbitrary boundary conditions", *Struct. Eng. Mech., Int. J.*, **35**(2), 217-240.
- Nayak, A.K., Moy, S.S.J. and Shenoi, R.A. (2002), "Free vibration analysis of composite sandwich plates based on Reddy's higher-order theory", *Compos. Part B: Eng.*, **33**(7), 505-519.
- Neves, A.M.A., Ferreira, A.J.M., Carrera, E., Cinefra, M., Roque, C.M.C., Jorge, R.M.N. and Soares, C.M.M. (2013), "Static, free vibration and buckling analysis of isotropic and sandwich functionally graded plates using a quasi-3D higher-order shear deformation theory and a meshless technique", *Compos. Part B: Eng.*, **44**(1), 657-674.
- Noor, A.K. (1973), "Free vibration of multilayered composite plates", *AIAA Journal*, **11**(7), 1038-1039.
- Noor, A.K., Burton, W.S. and Bert, C.W. (1996), "Computational models for sandwich panels and shells", *Appl. Mech. Reviews*, **49**(3), 155-199.
- Pagano, N.J. (1970), "Exact solutions for rectangular bidirectional composites and sandwich plates", *J. Compos. Mater.*, **34**, 20-34.
- Pai, P.F. and Schulz, M.J. (1999), "Shear correction factors and an energy-consistent beam theory", *Int. J. Solids Struct.*, **36**(10), 1523-1540.
- Peković, O., Stupar, S., Simonović, A., Svorcan, J. and Komarov, D. (2014), "Isogeometric bending analysis of composite plates based on a higher-order shear deformation theory", *J. Mech. Sci. Technol.*, **28**(8), 3153-3162.
- Phung-Van, P., Nguyen-Thoi, T., Bui-Xuan, T. and Lieu-Xuan, Q. (2015a), "A cell-based smoothed three-node Mindlin plate element (CS-FEM-MIN3) based on the C0-type higher-order shear deformation for geometrically nonlinear analysis of laminated composite plates", *Computat. Mater. Sci.*, **96**(B), 549-558.
- Phung-Van, P., De Lorenzis, L., Thai, C.H., Abdel-Wahab, M. and Nguyen-Xuan, H. (2015b), "Analysis of laminated composite plates integrated with piezoelectric sensors and actuators using higher-order shear deformation theory and isogeometric finite elements", *Computat. Mater. Sci.*, **96**(B), 495-505.



- Reddy, J.N. (1979), "Free vibration of antisymmetric angle-ply laminated plates including transverse shear deformation by the finite element method", *J. Sound Vib.*, **66**(4), 565-576.
- Reddy, J.N. (1997), *Mechanics of Laminated Composite Plates*, CRC Press, New York, NY, USA.
- Reddy, J.N. (2006), *Theory and Analysis of Elastic Plates and Shells*, CRC Press, Boca Raton, FL, USA.
- Reissner, E. (1972), "A consistent treatment of transverse shear deformations in laminated anisotropic plates", *AIAA Journal*, **10**(5), 716-718.
- Reissner, E. and Stavsky, Y. (1961), "Bending and stretching of certain types of heterogeneous anisotropic elastic plates", *J. Appl. Mech.*, **28**(3), 402-408.
- Swaminathan, K. and Patil, S.S. (2008a), "Higher order refined computational models for the free vibration analysis of antisymmetric angle-ply plates", *J. Reinf. Plast. Compos.*, **27**(5), 541-553.
- Swaminathan, K. and Patil, S.S. (2008b), "Analytical solutions using a higher order refined computational model with 12 degrees of freedom for the free vibration analysis of antisymmetric angle-ply plates", *Compos. Struct.*, **82**(2), 209-216.
- Thai, C.H., Nguyen-Xuan, H., Bordas, S.P.A., Nguyen-Thanh, N. and Rabczuk, T. (2015), "Isogeometric analysis of laminated composite plates using the higher-order shear deformation theory", *Mech. Adv. Mater. Struct.*, **22**(6), 451-469.
- Tran, L.V., Nguyen-Thoi, T., Thai, C.H. and Nguyen-Xuan, H. (2015), "An edge-based smoothed discrete shear gap method using the  $C^0$ -type higher-order shear deformation theory for analysis of laminated composite plates", *Mech. Adv. Mater. Struct.*, **22**(4), 248-268.
- Vinson, J.R. (2001), "Sandwich structures", *Appl. Mech. Reviews*, **54**, 201-214.
- Viswanathan, K.K. and Lee, S.K. (2007), "Free vibration of laminated cross-ply plates, including shear deformation by spline method", *Int. J. Mech. Sci.*, **49**(3), 352-363.
- Wang, X. and Shi, G. (2015), "A refined laminated plate theory accounting for the third-order shear deformation and interlaminar transverse stress continuity", *Appl. Math. Model.*, **39**(18), 5659-5680.
- Yang, H.T.Y., Saigal, S., Masud, A. and Kapania, R.K. (2000), "A survey of recent shell finite elements", *Int. J. Numer. Method. Eng.*, **47**(1-3), 101-127.
- Yang, Z., Chen, X., Zhang, X. and He, Z. (2013), "Free vibration and buckling analysis of plates using B-spline wavelet on the interval Mindlin element", *Appl. Math. Model.*, **37**(5), 3449-3466.
- Zhen, W. and Wanji, C. (2006), "Free vibration of laminated composite and sandwich plates using global-local higher-order theory", *J. Sound Vib.*, **298**(1-2), 333-349.
- Zuo, H., Yang, Z., Chen, X., Xie, Y. and Zhang, X. (2014), "Bending, free vibration and buckling analysis of functionally graded plates via wavelet finite element method", *Comput. Mater. Continua*, **44**(3), 167-204.
- Zuo, H., Yang, Z., Chen, X., Xie, Y. and Miao, H. (2015), "Analysis of laminated composite plates using wavelet finite element method and higher-order plate theory", *Compos. Struct.*, **131**(1), 248-258.

**Appendix**

$$\begin{aligned}
L_{11} &= \frac{d^2}{dX^2} - s_{10}\beta^2 + \lambda^2 & L_{12} &= (s_2 + s_{10})\beta \frac{d}{dX} \\
L_{13} &= -3s_{33}c_1\beta \frac{d^2}{dX^2} + s_{34}c_1\beta^3 & L_{14} &= 2(s_{15} - s_{33}c_1)\beta \frac{d}{dX} \\
L_{15} &= (s_{15} - s_{33}c_1) \frac{d^2}{dX^2} - (s_{16} - s_{34}c_1)\beta^2
\end{aligned} \tag{A1}$$

$$\begin{aligned}
L_{21} &= -(s_{10} + s_2)\beta \frac{d}{dX}, & L_{22} &= s_{10} \frac{d^2}{dX^2} - s_3\beta^2 + \lambda^2 \\
L_{23} &= -s_{33}c_1 \frac{d^3}{dX^3} + 3s_{34}c_1\beta^2 \frac{d}{dX}, & L_{24} &= (s_{15} - s_{33}c_1) \frac{d^2}{dX^2} - (s_{16} - s_{34}c_1)\beta^2 \\
L_{25} &= -2(s_{16} - s_{34}c_1)\beta \frac{d}{dX}
\end{aligned} \tag{A2}$$

$$\begin{aligned}
L_{31} &= -3s_{33}c_1\beta \frac{d^2}{dX^2} + s_{34}c_1\beta^3 & L_{32} &= s_{33}c_1 \frac{d^3}{dX^3} - 3s_{34}c_1\beta^2 \frac{d}{dX} \\
L_{33} &= -s_{23}c_1^2 \frac{d^4}{dX^4} + (2s_{24}c_1^2\beta^2 + 4s_{28}c_1^2\beta^2 + s_{14} - 2s_{30}c_2 + s_{32}c_2^2) \frac{d^2}{dX^2} \\
&\quad - (s_{25}c_1^2\beta^4 + s_{13}\beta^2 - 2s_{29}c_2\beta^2 + s_{31}c_2^2\beta^2) - c_1^2\lambda^2 p_3 \frac{d^2}{dX^2} + (\lambda^2 + c_1^2\lambda^2 p_3\beta^2) \\
L_{34} &= (s_{20}c_1 - s_{23}c_1^2) \frac{d^3}{dX^3} - (2s_{27}c_1\beta^2 - 2s_{28}c_1^2\beta^2 + s_{21}c_1\beta^2 \\
&\quad - s_{24}c_1^2\beta^2 - s_{14} + 2s_{30}c_2 - s_{32}c_2^2) \frac{d}{dX} + (c_1\lambda^2 p_2 - c_1^2\lambda^2 p_3) \frac{d}{dX} \\
L_{35} &= -(s_{21}c_1 - s_{24}c_1^2 + 2s_{27}c_1 - 2s_{28}c_1^2)\beta \frac{d^2}{dX^2} \\
&\quad + (s_{22}c_1\beta^3 - s_{25}c_1^2\beta^3 - s_{13}\beta + 2s_{29}c_2\beta - s_{31}c_2^2\beta) - (c_1\lambda^2 p_2\beta - c_1^2\lambda^2 p_3\beta)
\end{aligned} \tag{A3}$$

$$\begin{aligned}
L_{41} &= -2(s_{15} - s_{33}c_1)\beta \frac{d}{dX} \\
L_{42} &= (s_{15} - s_{33}c_1) \frac{d^2}{dX^2} - (s_{16} - s_{34}c_1)\beta^2 \\
L_{43} &= (s_{23}c_1^2 - s_{20}c_1) \frac{d^3}{dX^3} - (s_{24}c_1^2\beta^2 - s_{21}c_1\beta^2 + 2s_{28}c_1^2\beta^2 - 2s_{27}c_1\beta^2 + s_{14} - 2s_{30}c_2 + s_{32}c_2^2) \frac{d}{dX} \\
&\quad - (c_1\lambda^2 p_2 - c_1^2\lambda^2 p_3) \frac{d}{dX}
\end{aligned} \tag{A4}$$

$$L_{44} = (s_7 - 2s_{20}c_1 + s_{23}c_1^2) \frac{d^2}{dX^2} - (s_{12}\beta^2 - 2s_{27}c_1\beta^2 + s_{28}c_1^2\beta^2 + s_{14} - 2s_{30}c_2 + s_{32}c_2^2) + (\lambda^2 p_1 - 2c_1\lambda^2 p_2 + c_1^2\lambda^2 p_3) \quad (A4)$$

$$L_{45} = -(s_8 - 2s_{21}c_1 + s_{24}c_1^2 + s_{21} - 2s_{27}c_1 + s_{28}c_1^2) \beta \frac{d}{dX}$$

$$L_{51} = (s_{15} - s_{33}c_1) \frac{d^2}{dX^2} - (s_{16} - s_{34}c_1) \beta^2, \quad L_{52} = 2(s_{16} - s_{34}c_1) \beta \frac{d}{dX}$$

$$L_{53} = (2s_{28}c_1^2 - 2s_{27}c_1 + s_{24}c_1^2 - s_{21}c_1) \beta \frac{d^2}{dX^2} - (s_{25}c_1^2\beta^3 - s_{22}c_1\beta^3 + s_{13}\beta - 2s_{29}c_2\beta + s_{31}c_2^2\beta) - (c_1\beta\lambda^2 p_2 - c_1^2\beta\lambda^2 p_3) \quad (A5)$$

$$L_{54} = (s_{12} - 2s_{27}c_1 + s_{28}c_1^2 + s_8 - 2s_{21}c_1 + s_{24}c_1^2) \beta \frac{d}{dX}$$

$$L_{55} = (s_{12} - 2s_{27}c_1 + s_{28}c_1^2) \frac{d^2}{dX^2} - (s_9\beta^2 - 2s_{22}c_1\beta^2 + s_{25}c_1^2\beta^2 + s_{13} - 2s_{29}c_2 + s_{31}c_2^2) + (\lambda^2 p_1 - 2c_1\lambda^2 p_2 + c_1^2\lambda^2 p_3)$$

where

$$\lambda^2 = \frac{I_0 \omega^2 a^2}{A_{11}}, \quad p_1 = \frac{I_2}{I_0 a^2},$$

$$p_2 = \frac{I_4}{I_0 a^2}, \quad p_3 = \frac{I_6}{I_0 a^2}$$

$$\beta = n\pi\phi$$

$$s_2 = \frac{A_{12}}{A_{11}}, \quad s_3 = \frac{A_{22}}{A_{11}}, \quad s_7 = \frac{D_{11}}{a^2 A_{11}}, \quad s_8 = \frac{D_{12}}{a^2 A_{11}}, \quad s_9 = \frac{D_{22}}{a^2 A_{11}}, \quad s_{10} = \frac{A_{66}}{A_{11}}, \quad s_{12} = \frac{D_{66}}{a^2 A_{11}}, \quad s_{13} = \frac{A_{44}}{A_{11}},$$

$$s_{14} = \frac{A_{55}}{A_{11}}, \quad s_{15} = \frac{B_{16}}{aA_{11}}, \quad s_{16} = \frac{B_{26}}{aA_{11}}, \quad s_{20} = \frac{F_{11}}{a^4 A_{11}}, \quad s_{21} = \frac{F_{12}}{a^4 A_{11}}, \quad s_{22} = \frac{F_{22}}{a^4 A_{11}}, \quad s_{23} = \frac{H_{11}}{a^6 A_{11}}, \quad s_{24} = \frac{H_{12}}{a^6 A_{11}},$$

$$s_{25} = \frac{H_{22}}{a^6 A_{11}}, \quad s_{27} = \frac{F_{66}}{a^4 A_{11}}, \quad s_{28} = \frac{H_{66}}{a^6 A_{11}}, \quad s_{29} = \frac{D_{44}}{a^2 A_{11}}, \quad s_{30} = \frac{D_{55}}{a^2 A_{11}},$$

$$s_{31} = \frac{F_{44}}{a^4 A_{11}}, \quad s_{32} = \frac{F_{55}}{a^4 A_{11}}, \quad s_{33} = \frac{E_{16}}{a^3 A_{11}}, \quad s_{34} = \frac{E_{26}}{a^3 A_{11}}$$